



Evaluation of Unified Model Rainfall Forecasts over the Western Ghats and North East states of India

Kuldeep Sharma¹, Sushant Kumar¹, Raghavendra Ashrit¹, Sean Milton², Ashis K. Mitra¹ and
Ekkattil N. Rajagopal¹

¹National Centre for Medium Range Weather Forecasting, A-50, Sector-62, Noida 201309

²Met Office, FitzRoy Road, Exeter Devon, EX1 3PB, United Kingdom

Correspondence to: Kuldeep Sharma (kuldeep@ncmrwf.gov.in)

Abstract

Prediction of heavy rains associated with orography is still a challenge, even for the most advanced state-of-art high-resolution Numerical Weather Prediction (NWP) modeling systems. The aim of this study is to evaluate the performance of UK Met Office Unified Model (UM) in predicting heavy and very heavy rainfall exceeding 80th and 90th percentiles which occurs mainly due to the forced ascent of air parcels over the mountainous regions of the Western Ghats (WGs) and North East (NE) – states of India during the monsoon seasons of 2007 to 2018. Apart from the major upgrades in the dynamical core of UM from New Dynamics (ND) to Even Newer Dynamics for General Atmospheric Modeling of the environment (ENDGame), the horizontal resolution of the model has been increased from 40 km and 50 vertical levels in 2007 to 10km and 70 vertical levels in 2018. In general, it is expected that the prediction of heavy rainfall events improves with increased horizontal resolution of the model. The evaluation based on verification metrics, including Probability of Detection (POD), False Alarm Ratio (FAR), Frequency Bias (Bias) and Critical Success Index (CSI), indicate that model rainfall forecasts from 2007 to 2018 have improved from 0.29 to 0.38 (CSI), 0.45 to 0.55 (POD) and 0.55 to 0.45 in the case of FAR over WGs for rainfall exceeding the 80th percentile (CAT-1) in the Day-1 forecast. Additionally, the Symmetric Extremal Dependence Index (SEDI) is also used with special emphasis on verification of extreme and rare events. SEDI also shows an improvement



from 0.47 to 0.62 and 0.16 to 0.41 over WGs and NE-states during the period of study, suggesting an improved skill of predicting heavy rains over the mountains. It has also been found that the improvement is consistent and comparatively higher over WGs than NE-states.

Key Words: Orographic rain, Unified Model, Categorical verification, extreme rain, rainfall forecast, NWP

1. Introduction

Orography is the primary cause of up-lift of air parcels together with convectively driven rainfall in mountainous regions (Flynn et al., 2017). The spells of heavy orographic rainfall may induce landslides and flash flooding which lead to tremendous damage to the lives, property, infrastructure, environment and local economy. One of the most tragic landslides occurred in Kedarnath (Uttarkhand, India) in 2013 which led to more than 1000 deaths and 61000 stranded (Dube et al., 2014). During the last decade, the number of landslide incidences over India has increased and it contributes 16% of all rainfall-triggered landslides in the global dataset (Froude and Petley, 2018). The accurate prediction of this heavy rainfall with enough lead time over mountains can help in mitigation and precautions towards rainfall induced disasters.

Forecasting of this orographically induced heavy rainfall is one of the most challenging problems for numerical weather prediction (NWP) models. This is because of the complexity of the meteorological phenomena occurring over the orographic regions and the difficulty of obtaining detailed and precise observational data sets. (Smith et al., 1997, Mecklenburg et al., 2000, Lin et al., 2001). This leads to the poor representation initial conditions required to run the NWP model (Panziera et al., 2011). However, there is a significant improvement in the forecasting skill of NWP models in recent times. Some of these improvements can be attributed to the increased horizontal and vertical resolutions as well as improved physics parameterization schemes



49 (Sharma et. al. 2017), while major credit to the substantial improvements in weather forecasting
50 goes to the sophisticated data assimilation systems which utilize the satellite data.

51 The Indian subcontinent is highly vulnerable to heavy rainfall events. Most of the heavy and
52 extreme rainfall events occur during the southwest monsoon season (June to September, JJAS).
53 Western Ghats (WGs), North-Eastern (NE) states (Assam, Meghalaya, Mizoram, Arunachal
54 Pradesh, Sikkim, Manipur and Tripura) of India and central India are the most prominent regions
55 of heavy rainfall (Pattanaik and Rajeevan 2010). Central India receives rainfall mainly due to the
56 Low Pressure Systems (LPS) and Monsoon Depressions (MD) that form over the Bay of Bengal
57 (BoB) and move towards the west north-westward during JJAS (Goswami et al 2006; Sikka,
58 2006; Ajaymohan et al., 2010; Krishnamurthy and Ajaymohan, 2010) and only on very few
59 occasions do these LPS and MD's move northwards to produce a significant amount of rainfall
60 over the NE states. The WGs and the NE states of India are regions characterized by steep
61 orography and the heavy rainfall in these regions are often due to forced ascent of air parcels
62 over the mountains. These two mountainous regions of India have the highest annual rainfall
63 (Rao, 1976, Parthasarathy et al., 1995). The WGs are aligned north-south along the western coast
64 of India extending from Gujarat to Kerala with a narrow zonal width and steep rising western
65 face with the highest peak (2.6 Km) named Anamudi and located in Kerala. The north-east
66 region is dominated by the Eastern Himalayan mountain range. Geographically, two-thirds of the
67 area is hilly terrain interspersed with valleys and plains. The mean summer monsoon rainfall
68 over NE-States is ~151.3 cm which is much larger than the all India average (86.5cm)
69 (Parthasarathy et al., 1995) making it a potential zone for hydropower.

70 The WGs plays a dominant role in modulating the southwest monsoon, which in turn modulates
71 the regional climate (Gunnell 1997), as its first encounter on landfall over India is with these



72 mountain chains. Evaluation of the operational Unified Model (UM) rainfall forecast over India,
73 using multiple monsoon seasons, is documented in two recent studies. Kuldeep et al, (2017)
74 report improved skill of predicting heavy rainfall (>2 and >5 cm/day) over India (Core Monsoon
75 Zone: 18–28N, 68–88E). In another study, Kuldeep et al (2019) document the spatial verification
76 of rainfall using Contiguous Rain Areas (CRA) method over different regions of India. Here,
77 evaluation of operational UM rainfall forecasts is focused on mountainous regions of India (over
78 WGs and NE-states). The study period extends over twelve monsoon seasons (2007-2018).
79 Evaluation is carried out with special emphasis on heavy rainfall. Unlike earlier studies, the
80 verification is based on quintile based rainfall thresholds rather than absolute rainfall amounts.
81 During 2007-18, there has been considerable interannual variability in the monsoon. India
82 Meteorological Department (IMD) reports show that during 2007,2008,2010 and 2011-13,
83 monsoon rainfall was above normal, while it was below normal during 2009 and 2014-18. The
84 rainfall events exceeding two thresholds, the 80th (hereafter CAT-1) and 90th percentiles
85 (hereafter CAT-2) have been chosen to verify the forecast produced by the UM. For verification
86 based on percentiles the fraction of events classified as ‘yes’ are identical for different locations
87 or times of the year (Hamill and Juras, 2006), regardless of whether the climatological means
88 and variances are large or small. The rationale for choosing these rainfall thresholds of CAT-1
89 and CAT-2 based on percentiles is discussed in section 4.

90 **2. Data and Methodology**

91 **2.1 Observed Data**

92 The availability of daily rainfall data for long climatological periods is crucial for understanding
93 the components and processes related to the Indian monsoon. Daily rainfall associated with
94 orography, low-pressure systems and monsoon depressions contribute significantly to the total



95 seasonal rainfall. Orography plays a crucial role; the validation of numerical models requires
96 accurate rainfall information over land and adjoining seas (Mitra et al., 2013). The major data
97 sources of the rainfall are rain gauge, radar and satellite estimates (Ebert et al., 2003; Mitra et al.,
98 2009). Although the rain gauge network is not evenly spread in space and often very sparse over
99 unpopulated regions, particularly in mountainous areas, rainfall measurements from rain gauges
100 remain the most reliable data sources over land as they have good time resolution and provide an
101 accurate estimate of ground truth at a particular location. The improved representation of heavy
102 rainfall events due to an enhanced rain gauge network over WGs and NE-states have been
103 recently reported in Pai et al. (2014).

104 The period of the observed dataset used in this study is the monsoon season (JJAS) from 2007 to
105 2018. The two domains selected for the study are WGs (72-78°E, 8-23°N) and NE- states (88-
106 100°E, 21-30°N). The verification has been carried out over Indian land points only.

107 The gridded daily rainfall data set obtained from IMD for the period 2007–2011 is used in the
108 present study. The geographical distribution of IMD's rain gauges on any typical day over India
109 during the monsoon is shown in Figure 1(a). The boxes (WGs and NE-states) represent the
110 domains chosen for this study. The zoomed plots of WGs and NE-states are also displayed in
111 Figure 1(b) and (c). The number of grid points (land only) over WGs and NE-states used in the
112 present study are 475 and 403 respectively. The number of rain gauge stations on any typical
113 day over WG and NE-states are 796 and 132 respectively. The Shepard interpolation technique
114 (1968), also discussed in Rajeevan et al. (2006), has been adopted for the gridding this rainfall
115 data. During the monsoon seasons of 2012-2018, NCMRWF-IMD (National Centre for Medium
116 Range Weather Forecasting - Indian Meteorological Department) merged satellite-rainfall
117 analyses have been used. For the monsoon seasons of 2012-15, NCMRWF-IMD rainfall data are



the merged product of near-real-time Tropical Rainfall Measuring Mission Multi-satellite Precipitation Analysis (TMPA)-3B42 and rain gauge data from the India Meteorological Department (IMD) using an objective analysis scheme (NMSG; Mitra et al. 2009). For the period 2016-2018, the rainfall estimates from Global Precipitation Measurement (GPM) satellite have been used to merge with IMD's rain gauge stations to characterize the best rainfall estimates over the Indian region. The spatial resolution of the data is at $0.5^\circ \times 0.5^\circ$. However, the spatial resolution of rainfall data from the monsoon season of 2016 onwards is available originally at a horizontal resolution of 0.25° , but we have interpolated this data set using a bilinear interpolation technique at a spatial resolution of 0.5° to make a uniform rainfall data series throughout the study. This merged data set represents the Indian monsoon rainfall more realistically and is superior to other available rainfall data sets over the Indian monsoon region because it uses additional local rain gauge observations (Mitra et al. 2013), and consequently provides a better baseline for NWP model validation and monsoon model development.

2.2 Description of the NWP Modelling System and Forecast Dataset

The Unified Model at the UK Met Office is the numerical modeling system developed for the seamless prediction of weather and climate systems (Davies et al. 2005; Brown et al. 2012, Wood et al. 2014; Met Office 2014). This 'seamless' prediction system implies that the same model with slightly different configurations (e.g. resolution) is used across a range of temporal and spatial scales, with configurations traceable to each other and designed to best represent the processes which have most influence on the timescale of interest (Martin et al. 2010). The rainfall forecast from the Met Office operational medium range (1-7 day) global model configuration is used in this study. The Unified Model (UM) is in a process of continuous development, taking advantage of improved understanding of atmospheric processes and steadily



141 increasing supercomputer power. The atmospheric component of the UM is based on non-
142 hydrostatic dynamics with semi-Lagrangian advection and semi-implicit time stepping. It is a
143 grid point model with the ability to run with a rotated pole and variable horizontal grid. A
144 number of sub-grid scale processes are represented, including convection (Gregory and
145 Rowntree 1990; Gregory and Allen 1991; Grant 2001), boundary layer turbulence (Brown et al.,
146 2007), radiation (Edwards and Slingo, 1996), cloud microphysics and orographic drag (Webster
147 et al.2003). The model is initialized using a state of the art global four-dimensional variation
148 (4DVAR; Rawlins et al. 2007) data assimilation technique. The year to year important changes
149 and upgrades during 2007–2018 in the model configuration are briefly listed in Table 1. During
150 2007–2018, the horizontal and vertical resolution of the global NWP configuration improved
151 from about 40 km and 50 levels in 2007 to about 10 km and 70 levels in 2018. A major upgrade
152 in the dynamical core happened in July 2014. In 2002 the “New Dynamics” upgrade was
153 implemented (Davies et al., 2005). After a decade, in July 2014, the new dynamical core named
154 “ENDgame” was implemented operationally at Met Office UM (Wood et al. 2014; Met
155 Office2014). The “ENDGame” has an advantage over its predecessor “New Dynamics” in terms
156 of increases in atmospheric variability. This is manifest in improved details and intensity of
157 large-scale storms in weather forecasts, which arises from the use of less artificial damping in the
158 ENDGame formulation (Met Office 2014). In addition to horizontal resolution and dynamical
159 core, a number of other key changes were introduced. One is the change of resolution of data
160 assimilation component from approximately 60 km (N216) to 40 km (N320). There is a change
161 to model physics which includes an increase in entrainment rate in deep convection and
162 improvements to several other physical parameterization schemes. The complete package is
163 called Global Atmosphere 6.0 (GA6) and more details are available in Walters et al. (2017).



164 Daily rainfall forecast up to Day-3, produced by the global operational UM used for NWP have
165 been evaluated over two mountainous regions of WGs and NE-states. The rainfall forecast is also
166 interpolated at $0.5^\circ \times 0.5^\circ$ for direct comparison with the observed rainfall. The evaluation has
167 been restricted only over the land points to focus the model performance over land orographic
168 regions.

169 **3. Verification Approach**

170 Traditional verification methods such as a categorical approach are generally based on rainfall
171 accumulation thresholds or rainfall ranges. This approach is used by most of the operational
172 NWP centers to evaluate the rainfall forecast (Airey and Hulme, 1995; Wilson, 2000). When we
173 consider a fixed rainfall threshold or range, it is observed that the verification scores drop quite
174 rapidly, particularly at high threshold or range (Ashrit et al., 2015). In general, the rainfall
175 distribution over different regions are inhomogeneous due to different precipitation mechanisms.
176 As discussed earlier about the occurrence of rainfall at different regions of India, it is very
177 difficult to choose the same threshold of absolute quantities to evaluate the skill of a model (in
178 different regions). For instance, a rainfall threshold of 5cm/day over the core monsoon Zone
179 (CMZ) can be considered as heavy rain (Sharma et al., 2017), which may not be the case over
180 the WGs and NE-states. There is a need to revisit rainfall verification based on accumulation
181 thresholds or ranges. To overcome this issue, Robert (2008) and Zhu et al. (2015) have used
182 rainfall verification based on percentiles rather than the accumulation thresholds. The purpose of
183 choosing the percentiles over accumulation thresholds is to remove the impact of any biases and
184 climatological frequencies for that region (Robert 2008; Zhu et al., 2002; Buizza et al., 2003). In
185 the present study, daily rainfall forecasts have been verified using the standard categorical



186 scores, for percentile-based thresholds. A categorical approach is based on the 2x2 contingency
187 table (Table 2) evaluating for different thresholds.

188 To evaluate the skill of the NWP forecast system, verification metrics focus on the
189 correspondence between the observation and forecast (Murphy, 1993). The 24-hour rainfall
190 exceeding 80th and 90th percentiles thresholds are events of interest in the present study. The
191 percentiles are computed over the entire period (2007-2018). Figure S1 (a) and (b) show 80th and
192 90th percentiles rainfall in the observations. Similarly, the bottom panels, Figure S1 (c) and (d)
193 show 80th and 90th percentiles rainfall in the forecasts. These are the reference thresholds for the
194 evaluation. A *hit* is considered when prediction of an event matches the observation on a grid
195 point, while an event on a grid point predicted but not observed, we denote as a *false alarm* (b).
196 A *miss* (c) occurs when an event is not predicted but is actually observed. Finally, *correct*
197 *rejection* (d) is when an event doesn't occur and the model doesn't predict it. These four
198 variables are the components of the 2x2 contingency table and are displayed in Table 2. BIAS,
199 Probability of Detection (POD), False Alarm Ratio (FAR), Critical Success Index (CSI) and
200 Symmetric Extremal Dependence Index (SEDI) are some of the metrics used in this study. POD
201 is defined as ratio of number of correct forecasts (a) to the number of observed events (a+c)
202 while FAR is the ratio of number of false alarms (b) to the number of forecasts made (a + b). The
203 ratio of number of hits (a) to all events either forecast or observed (a + b + c) is known as CSI.
204 All three scores range from 0 to 1, with 1 being a perfect score in case of POD as well as CSI
205 and 0 for perfect FAR. The Bias Score is calculated as the ratio of the number of predicted
206 events (a+b) to the observed events (a+c) exceeding a given threshold (Donaldson et al., 1975).
207 The Bias Score ranges from 0 to infinity with a value of 1 meaning perfect forecast. The Bias
208 Score can help in identifying whether the forecast system has a tendency to underpredict



(BIAS<1) or overpredict (BIAS>1) events. Since the Bias Score does not provide any information about the forecast accuracy, it is generally evaluated in conjunction with another verification score such as Critical Success Index (CSI) or Equitable Threat Score (ETS) (Ebert et al 2003). The detailed formulae of these metrics are displayed in Table 3 and a detailed description can be found in Wilks (2011) and Jolliffe and Stephenson (2012). These verification metrics have been computed for twelve monsoon seasons for rainfall exceeding 80th (CAT-1) and 90th percentiles (CAT-2) over WGs and NE-states.

4. Results and Discussion

4.1. Evaluation of Forecast Rain during recent years

The mean seasonal rainfall obtained from observations and Day-3 forecast of the UM along with Mean Error (ME) over the Indian region for 2013, 2015 and 2018 is shown in the Figure 2. The boxes represent the area of study used for categorical verification. We have evaluated the rainfall for Day-1, Day-2 and Day-3 forecast but the results are shown only for Day-3 forecast for brevity. The monsoon seasons of 2013, 2015 and 2018 are chosen to highlight the improvement in mean rainfall forecast due to increasing the horizontal resolution and major model upgrades discussed in section 2.2. During JJAS of 2013 and 2015, the UM's horizontal resolution was N512 (~25km) and N768 (~17km) respectively while the dynamical core was upgraded from New Dynamics to ENDgame. Further, the model underwent increased horizontal resolution of N1280 (~10km) during JJAS 2018. Although, we have evaluated the rainfall forecast for earlier seasons during 2007-2012 also, but no significant change is found over WGs and NE-states compared to N512 in capturing the monsoon rainfall.

As discussed, forecasting of rainfall in the tropics and Indian region, especially over the mountainous regions of WGs and NE-states, is always a challenge. However, the NWP models



are capable of capturing the large-scale features, but again these models also fail to pick up the fine scale features on many occasions. The UM Day-3 forecasts successfully predict the mean high rainfall amounts along WGs with a reducing rainfall eastwards over the peninsular India, while for rainfall over the NE-states, the model consistently shows over prediction during the monsoon seasons of 2013, 2015 and 2018. This is quantified in terms of ME showing a wet bias in the NE-States (extreme right panel Figure 2c, 2f, 2i). This wet bias has also been observed in other monsoon seasons. The model shows a large wet bias in rainfall over the Indo-Gangetic region adjoining the Himalayas during JJAS 2013, which is improved after 2013 as seen during the monsoon seasons of 2015 and 2018. One of the possible reasons for the improvement in the rainfall forecast over the Indo-Gangetic plains is the reduction in the UM bias for too strong easterlies at 850 hPa (Iyengar et al., 2011) (Please see S2).

4.2.Evaluation of Peak rainfall Forecast during recent years

The highest rainfall of the monsoon season of 2013, 2015 and 2018 at each grid point over the Indian regions is shown in Figure 3 from observed and model Day-3 rainfall forecasts. The top panel shows the observed highest daily rainfall during respective seasons (Figure 3a, b and c) while the bottom panel shows the Day-3 highest rainfall predicted by UM (Figure 3d, e and f). During JJAS 2013, UM in Day-3 forecast fails to achieve the highest rainfall of the season (Figure 3d) as compared to observed peak rainfall (Figure 3a) over the WGs. This is substantially improved in 2015 and 2018 monsoon seasons as evident in the Figure (3b, e) and Figure (3c, f). Although, the model also shows some false alarms in this region, it consistently retains the peak amount of rainfall in Day-3 forecasts over the NE-states. Figures 4 (a) and (b) show the rainfall counts (>10cm/day) in observations and Day-3 forecasts over WGs and NE-states. Over WGs, the number of counts consistently increased in Day-3 forecasts after 2011 and



255 it has reached closer to the observed counts in 2018 (Figure 4a). During 2008 and 2009, the
256 model over-predicts the counts of rainfall exceeding 10cm/day. The number of counts has
257 increased over NE-states also except 2012 and 2013. The model gives an indication of over-
258 estimation in picking up these counts in the rest of these years (Figure 4b). The improvement in
259 mean rainfall (section 4.1) and highest rainfall is linked to the improved horizontal resolution in
260 model and data assimilation system as well as the upgrade of the dynamical core from New
261 Dynamics (ND) to ENDgame. Also, the revised physics package including the increase in
262 entrainment rate in deep convection together with improvements to several other physical
263 parameterization schemes lead to the improvement in the skill of UM rainfall forecast (Walters et
264 al. 2017. Sharma et al 2017).

265 **4.3.Number of counts of rainfall exceeding 80th and 90th percentiles**

266 As discussed before, the 80th and 90th percentile thresholds correspond to entire period 2007 to
267 2018. For each monsoon season, we calculate the grid point counts exceeding these thresholds as
268 shown in Figure 5(a) and (b). For NE, there are 475x122 grids and WG there are 403x122 grid
269 point counts. It is evident in Figure 5(a) that the number of grid point counts of rainfall
270 exceeding 80th percentiles (CAT-1) is varying from 2000 to 4000 over WG. Similarly, over NE-
271 states, this count varies from 1800 to 2500. Similarly, for 90th percentile threshold (CAT-2) the
272 counts vary from 1100 to 2100 over WG and 500 to 1500 over NE. These counts form good
273 sample sizes for evaluation the rainfall exceeding 80th and 90th percentiles.

274 **4.4.Rainfall forecast verification over WGs and NE-states using traditional verification** 275 **metrics**

276 Figures 6 and 7 display the seasonal verification scores of four metrics (BIAS, POD, FAR and
277 CSI) computed based on the 2x2 contingency table for two rainfall thresholds of CAT-1 and



278 CAT-2 over WGs and NE-states respectively. Day-1, Day-2 and Day-3 forecast have been
279 chosen for evaluation. It is evident from figures 6 and 7 that the prediction of orographic rainfall
280 during the monsoon seasons of 2007 to 2018 has been improved up to Day-3 of the forecasts
281 over both the regions of study for the chosen thresholds of CAT-1 and CAT-2. However, the
282 seasonal CSI values show a decrease with increase threshold for Day-1 to Day-3 forecasts
283 (Figures 6 and 7(j-l)). While analyzing the model's performance over both the mountainous
284 regions, CSI has a higher magnitude over WGs compared to NE-states for CAT-1 and CAT-2
285 thresholds.

286 A consistent increase (decrease) in POD (FAR) for both the rainfall thresholds of CAT-1 and
287 CAT-2 at all lead times clearly indicates the improvement in UM's performance in predicting
288 heavy (CAT-1) and very heavy rainfall (CAT-2) events over both the regions affected by
289 orographic rainfall (Figure 6(d-f) and 7 (d-f)). This indicates the hit rate has increased during
290 these monsoon years at both the rainfall thresholds of CAT-1 and CAT-2. This increase in hit
291 rate is due to more events being correctly predicted (Sukovich et al., 2014). Also, the reduction
292 in FAR indicates the improvement in POD is also due to a more accurate forecast rather than a
293 'spurious' increase in the number of extreme forecasts being made. This confirms that the
294 improvement in skill of rainfall forecast of UM during the twelve monsoon seasons is genuine
295 and not an artifact of more extreme rainfall forecasts being issued or the choice of verification
296 metrics.

297 The seasonal verification of frequency BIAS during JJAS 2007 to 2018 are presented in Figures
298 6 and 7 (a-c) over both the mountainous regions of WGs and NE-states respectively for Day-1 to
299 Day-3 forecast. The model accurately predicts these events of CAT-1 and CAT-2 at all lead
300 times during 2007 to 2018. Since the Bias Score does not provide any information about the



301 forecast accuracy, it is generally evaluated in conjunction with another verification score such as
302 Critical Success Index (CSI) which provide additional information (Ebert et al., 2003).

303 **4.5. Improvement in rainfall forecast : Extreme scores**

304 Although the traditional verification scores such as CSI discussed in previous sections depict an
305 improvement in the UM global operational NWP forecasting system during recent years, it tends
306 to zero for rare events due to its low frequency of occurrence. Consequently, the assessment of
307 the skill of forecasting of such heavy rainfall events is problematic because of the rarity of such
308 events. The verification using these categorical scores (e.g CSI, ETS, and POD) creates a
309 misleading impression that rare events cannot be skillfully forecast irrespective of the forecasting
310 system (Stephenson et al., 2008). To overcome the shortcomings of the traditional verification
311 metrics in predicting rare events, Ferro and Stepheson (2011) proposed a new set of verification
312 metrics named the Extremal Dependence Index (EDI) and Symmetric EDI (SEDI). These scores
313 range from -1 to 1 with 0 measuring no skill and 1 measuring the perfect score. The main
314 advantages in these verification metrics are their independence of the base rate and the fact that they
315 do not converge to trivial values even at high rainfall events (rare events). SEDI verification
316 metrics for two thresholds of CAT-1 and CAT-2 during the twelve monsoon seasons are
317 displayed in Figure 7 (a-c) and 8 (a-c) over WGs and NE-states at all lead times. It is clear from
318 Figures 8 and 9 that the skill of the model has improved in predicting heavy rainfall (CAT-1) and
319 very heavy rainfall events (CAT-2) during the recent monsoon seasons and at all forecast lead
320 times. Also, the magnitude of SEDI is higher compared to traditional verification metrics (CSI)
321 used in the previous section. Some of the recent improvement in the UM rainfall forecast over
322 the mountains can be attributed to increased horizontal resolution along with improved physics
323 schemes and data assimilation. A significant improvement is also evident from 2007 to 2008.



324 This improved skill is due to the upgrades in data assimilation system which had a full
325 implementation of perturbed forecast physics convection, soil moisture nudging and increase
326 vertical range of GPSRO data assimilation.

327 **Summary and Conclusions**

328 During the monsoon season, heavy rainfall events over the orographic regions of WGs and NE-
329 states of India pose a great challenge to accurate prediction using NWP models. This is mainly
330 due to the medium and coarser grid resolution models, which fail to accurately resolve the
331 orographic features and related meteorological processes. While increased grid resolution
332 improves heavy rainfall prediction, it often leads to forecasting excessive and unrealistic rainfall
333 associated with the mountains. The work reported in this paper evaluates and documents the
334 improved skill in the Met Office Unified Model (UM) operational global NWP rainfall forecasts
335 over the hilly regions of India during the monsoon seasons of 2007-2018. The changes in the
336 operational UM during 2007-2018 include improvements in the representation of physical
337 processes, improved dynamics and increased grid resolution from about 50km in 2007 to 10km
338 in 2018. It is rather crucial to identify and quantify the impact of improved grid resolution in
339 improved skill of the forecast model in predicting the heavy rains over hilly regions which are
340 responsible for flash floods and landslides.

341 Evaluation results show that UM forecasts successfully capture all the large-scale monsoon
342 rainfall features. The typical high rainfall amounts along the WGs and reducing rainfall amounts
343 eastwards over the Indian peninsula is realistic. Similarly, high rainfall amounts over the North
344 Eastern States with progressively reduced amounts westwards are also accurate. Evaluation
345 suggests some of the following significant improvements during 2007-2018.



346 • The large wet bias over northern India adjoining the Himalayas during 2013 is
347 significantly reduced during JJAS 2015 and 2018.

348 • The highest observed rainfall amounts over WGs (>10cm/day) are completely missed in
349 the forecasts during JJAS 2013. Following improved grid resolution and move to
350 ENDGAME dynamical core in 2014, both of which improved the synoptic variability in
351 the UM forecasts, the observed peak rainfall amounts (>10cm/day and also >20cm/day)
352 are better predicted along the west coast of India during JJAS 2015 and 2018.

353 The verification carried out with focus on heavy (CAT-1; >80th percentile) and very heavy
354 rainfall (CAT-2; > 90th percentile) forecasts adopts a method that takes into account the spatial
355 variations in climatological characteristics. The main conclusions are-

356 • Rainfall forecast for CAT-1 has been improved by 0.18 to 0.34 (0.14 to 0.23), 0.3 to 0.5
357 (0.25 to 0.37) and 0.7 to 0.5 (0.75 to 0.62) in the case of CSI, POD and FAR respectively
358 from 2007 to 2018 over WGs (NE-states) in Day-3 forecast. Also, CSI, POD and FAR
359 indicate an improvement from 0.1 to 0.24 (0.08 to 0.15), 0.18 to 0.38 (0.15 to 0.26) and
360 0.81 to 0.61 (0.84 to 0.73) for CAT-2 over WGs (NE-states). Improved skill over the
361 WG's is higher compared to that in NE-states.

362 • Further, verification metrics (SEDI) for extreme and rare events have also been
363 computed. An increase in SEDI from 0.21 to 0.55 (0.10 to 0.33) in Day-3 forecast has
364 been noted over WGs (NE-states) in SEDI for CAT-1. The improvement in SEDI is quite
365 impressive and is 0.19 to 0.51 (0.12 to 0.32) over WGs (NE-states) for CAT-2.

366 This study is based on the long record (2007-2018) of UM global model's real time rainfall
367 forecasts over India to highlight the improved skill in heavy rainfall forecasts. More recently



high-resolution NWP models are being used in India for operational forecasts of heavy rainfall events. Global 12km grid deterministic (NCUM) and Ensemble (NEPS; 23 members) are operational at NCMRWF. These models are also being evaluated for each season (Ashrit et al 2018) based on the 0.25 x 0.25 grid IMD-NCMRWF merged (Gauge + Satellite) rainfall analysis used in this study since higher resolution satellite-based products have biases over land and fail to capture heavy rains over land (Mitra et al., 2013). Very high resolution rainfall analysis based on all conventional rain gauges, DWR and Satellite is essential for systematic evaluation of the heavy rainfall forecasts over India.

Code and Data Availability:

The verification carried out in the present study uses Fortran Codes, R-Software and verification package available in R. The observed daily rainfall data and the codes used in the study is available at <ftp://ftp.ncmrwf.gov.in/pub/outgoing/kuldeep/GMED>. National Center for Medium Range Weather Forecasting (NCMRWF) has an MoU with Met Office, Exeter. This Unified Model (UM) forecast data can't be shared as we do receive this dataset under the mutual collaboration. However, the UM data is available for registered users on TIGGE portal (<https://apps.ecmwf.int/datasets/data/tigge/levtype=sfc/type=pf/>)

Author's Contribution:

To bring the manuscript in the final form, KS and RA have designed the approach of evaluation of rainfall skill over the orographic regions of India. The analysis has been carried out by KS and SK. AKM is the one who has developed the observed rainfall (Merged product) used in this study. ENR and SM are the principal scientists for the collaboration between NCMRWF and Met Office. KS and SK have finalized the manuscript with contributions of all the authors.



390 Acknowledgements

391 This work and its contributor Sean Milton were supported by the Met Office Weather and
392 Climate Science for Service Partnership (WCSSP) India as part of the Newton Fund.

393 References

- 394 Airey, M. and Hulme, M.: Evaluating climate model simulations of precipitation: methods,
395 problems and performances. *Progress in Physical Geography*, 19, 427-448, 1995.
- 396 Ajayamohan, R.S., Merryfield, W. J., and Kharin, V.V.: Increasing trend of synoptic activity
397 and its relationship with extreme rain events over central India. *J. Clim.*, 23, 1004-1013, 2010.
398
- 399 Ashrit, R., Sharma, K., Dube, A., Iyengar, G.R., Mitra, A.K. and Rajagopal, E.N.: Verification of
400 short-range forecasts of extreme rainfall during monsoon. *Mausam*, 66, 375-386, 2015.
401
- 402 Ashrit, R. et al.: Performance of NCMRWF Unified Model during the South-West Monsoon
403 2017. Chapter 11, Monsoon A Report 2017, IMD Met Monograph: No.: ESSO/IMD/Synoptic
404 Met./01(2018)/22, 2018.
405
- 406 Brown, A.R., Beare, R.J., Edwards, J.M, Lock, A.P., Keogh, S.J., Milton, S.F., and Walters,
407 D.N.: Upgrades to the boundary layer scheme in the Met Office NWP model. *Bound. Lay.*
408 *Meteorol.*, 118, 117-132, 2007.
- 409 Brown, A., Milton, S., Cullen, M., Golding, B., Mitchell, J. and Shelly, A.: Unified Modeling
410 and Prediction of Weather and Climate: A 25-Year Journey. *Bull. Amer. Met. Soc.*, 93, 1865–
411 1877, 2012.
- 412 Buizza, R., Richardson, D. S. and Palmer, T. N. Benefits of increased resolution in the ECMWF
413 ensemble prediction system and comparison with poor-man’s ensembles. *Q. J. R. Meteorol. Soc.*,
414 129, 1269–1288, 2003.
- 415 Davies, T., Cullen, M. J. P., Malcom, A. J., Mawson, M. H., Staniforth, A., White, A. A. and
416 Wood, N.: A new dynamical core for the Met Office’s global and regional modeling of the
417 atmosphere. *Q. J. R. Meteorol. Soc.*, 131, 759–1782 2005.
- 418 Dube, A., Ashrit, R., Ashish, A., Sharma, K., Iyengar, G.R., Rajagopal, E.N. and Basu, S.:
419 Forecasting the heavy rainfall during Himalayan flooding—June 2013. *Wea. Cli. Extremes.*, 4, 22–
420 34, 2014.
- 421 Ebert, E.E., Damrath, U., Wergen, W. and Baldwin, M.E.: The WGNE assessment of short-term
422 quantitative precipitation forecasts. *Bull. Amer. Met. Soc.*, 84, 481-492, 2003.



- 423
424 Edwards, J.M. and Slingo, A.: Studies with a flexible new radiation code Part I. Choosing a
425 configuration for a large-scale model. *Q. J. R. Met. Soc.*, 122, 689–719, 1996.
- 426 Ferro, C.A.T. and Stephenson, D. B.: Extremal dependence indices: improved verification
427 measures for deterministic forecasts of rare binary events. *Wea. Forecasting.*, 26, 699–713,
428 2011.
- 429 Flynn, W. J., Nesbitt, S. W., Anders, A. M., and Garg, P.: Mesoscale precipitation characteristics
430 near the Western Ghats during the Indian Summer Monsoon as simulated by a high-resolution
431 regional model. *Q.J.R. Meteorol. Soc.*, 143, 3070–3084, 2017.
- 432
433 Froude, M., J. and Petley, D.,N.: Global fatal landslide occurrence from 2004 to 2016.*Nat.*
434 *Hazards Earth Syst. Sci.*, 18, 2161–2181, 2018.
- 435
436 Goswami, B.N., Venugopal, V., Sengupta, D., Madhusoodanan, M.S. and Xavier P.K.:
437 Increasing trend of extreme rain events over India in a warming environment.*Science*.314,1442-
438 1445, 2006.
- 439
440 Gregory, D. and Rowntree, P.R.: A mass flux convection scheme with representation of cloud
441 ensemble characteristics and stability dependent closure.*Mon. Wea. Rev.*, 118,1483-1506, 1990.
- 442 Gregory, D. and Allen, S. (1991). The effect of convective scale downdraughts upon NWP and
443 Climate. Proc. 9th AMS conf on NWP, Denver, USA, 122-123.
- 444 Gunnell, Y. (1997).: Relief and climate in South Asia: the influence of the Western Ghats on the
445 current climate pattern of peninsular India. *Int J Climatol.* 17,1169–1182, 1997.
- 446 Hamill, T.M. and Juras, J.: Measuring forecast skill: is it real skill or is it the varying
447 climatology? *Q. J. R. Meteorol. Soc.*, 132, 2905–2923, 2006.
- 448 Iyengar, G., Ashrit, R., Dasgupta, M. M., Chourasia, M., Sharma, K., Prasad, V. S., Rajagopal,
449 E. N., Mitra, A.K., Mohandas, S. and Harenduprakash, L.: NCMRWF &UKMO Global Model
450 forecast verification: Monsoon 2010. *NCMRWF Research Report*.NMRF/MR/02/2011, 2010.
- 451 Jolliffe, I.T. and Stephenson, D.B.: Forecast Verification: A Practitioner's Guide in Atmospheric
452 Science, Second Edition (eds I. T. Jolliffe and D. B. Stephenson), John Wiley & Sons, Ltd,
453 Chichester, West Sussex, PO19 8SQ, UK, 2012.
- 454 Krishnamurthy, V. and Ajayamohan, R. S.: Composite Structure of monsoon low-pressure
455 systems and its relation to Indian rainfall.*J. Climate.*,23, 4285–4305, 2010.
- 456 Lin, Y.L., Chiao, S., Wang, T.A., Kaplan,M.L., Weglarz, R.P.: Some Common Ingredients for
457 Heavy Orographic Rainfall, *Wea. Forecasting.*,16, 633-660, 2001.



- 458 Martin, G.M., Milton, S.F., Senior, C.A., Brooks, M.E., Ineson, S., Reichler, T., Kim, J.:
459 Analysis and Reduction of Systematic Errors through a Seamless Approach to Modeling
460 Weather and Climate. *J. Climate* 23, 5933–5957, 2010.
- 461 Mecklenburg, S., Joss, J., and Schmid W.: Improving the nowcasting of precipitation in an
462 Alpine region with an enhanced radar echo tracking algorithm. *J. Hydrol.* 239, 46–68, 2000.
- 463 Met Office,: ENDGame: A new dynamical core for seamless atmospheric prediction. Available
464 at <http://www.metoffice.gov.uk/research/news/2014/endgame-a-new-dynamical-core>, 2014.
- 465 Mitra, A.K., Bohra, A.K., Rajeevan, M.N. and Krishnamurti, T.N.(2009). Daily Indian
466 precipitation analyses formed from a merge of rain-gauge with TRMM TMPA satellite-derived
467 rainfall estimates. *J. Meteor. Soc. of Japan*, 87A, 265-279.
- 468 Mitra, A.K., Momin, I.M., Rajagopal, E.N., Basu, S., Rajeevan, M.N. and Krishnamurti, T.N.
469 (2013). Gridded daily Indian monsoon rainfall for 14 seasons: Merged TRMM and IMD gauge
470 analyzed values. *Journal of Earth System Science*, 122(5),1173-1182
- 471 Murphy, A.H. (1993). What is a good forecast? An essay on the nature of goodness in weather
472 forecasting. *Wea. Forecasting.*, 8, 281–293.
- 473 Pai, D.S., Sridhar, L., Rajeevan, M., Sreejith, O.P., Satbhai, N.S., and B. Mukhopadhyay (2014).
474 Development of a new high spatial resolution ($0.25^\circ \times 0.25^\circ$) long period (1901-2010) daily
475 gridded rainfall data set over India and its comparison with existing data sets over the region.
476 *Mausum*,65,1-18.
- 477 Panziera, L.,Germann, U., Gabella, M. and P. V. Mandapaka (2011). NORA–Nowcasting of
478 Orographic Rainfall by means of Analogues. *Q.J.R. Meteorol. Soc.*, 137, 2106–2123.
- 479 Parthasarathy, B., Munot, A. A. andKothawale, D. R. (1995). Monthly and seasonal time series
480 for all India, homogeneous regions and meteorological subdivisions: 1871–1994, *Res. Rep.*
481 *RR-065*, 113 pp., Indian Institute of Tropical Meteorology, Pune, India.
- 482 Pattanaik, D. R. and Rajeevan, M.N.(2010). Variability of extreme rainfall events over India
483 during southwest monsoon season.*Meteorol. Appl.*17, 88-104.
484
- 485 Rajeevan,M., Bhate, J. , Kale, J. D. and Lal, B. (2006).High resolution daily gridded rainfall data
486 for the Indian region: Analysis of break and active monsoon spells.*Current Science*, VOL. 91,
487 NO. 3, pp. 296-306.
- 488 Rao, Y.P. (1976). Southwest monsoon; meteorological monograph, synoptic meteorology, No
489 1/1976, India Meteorological Department
490



- 491 Rawlins, F., Ballard, S. P., Bovis, K.J., Clayton, A. M., Li, D., Inverarity, G.W., Lorenc, A.C. and
492 Payne, T.J. (2007). The Met Office global four dimensional variational data assimilation scheme,
493 *Q. J. R. Meteorol. Soc.*, 133, 347–362
- 494 Roberts, N. (2008). Assessing the spatial and temporal variation in the skill of precipitation
495 forecasts from an NWP model, *Meteorol. Appl.*, 15, 163–169
- 496 Sharma, K., Ashrit, R., Bhatla, R., Mitra, A.K., Iyengar, G.R. and Rajagopal, E.N. (2017). Skill
497 of Predicting Heavy Rainfall Over India: Improvement in Recent Years Using UKMO Global
498 Model. *Pure appl. geophys.*, 174, 4241–4250.
- 499 Shepard D. : A two-dimensional interpolation function for irregularly spaced data. In Proceedings
500 of the 23rd ACM National Conference, New York, USA, 27–29 August 1968, 1968.
- 501 Sikka, D.R.: A Study on the Monsoon Low-Pressure Systems over the Indian region and their
502 relationship with drought and excess monsoon seasonal rainfall. *COLA Technical Report 217*.
503 USA, 61pp, 2006
- 504 Smith, R.B., and Coauthors: Local and remote effects of mountains on weather: Research needs
505 and opportunities. *Bull. Amer. Meteor.* 78, 877–892, 1997.
- 506 Stephenson, D.B., Casati, B., Ferro, C.A.T. and Wilson, C.A.: The Extreme Dependency Score:
507 a non-vanishing measure for forecasts of rare events. *Meteorol. Appl.*, 15, 41–50, 2008
- 508 Sukovich, E.M., Ralph, F.M., Barthold, F.E., Reynolds, D.W. and Novak, D.R.: Extreme
509 Quantitative Precipitation Forecast Performance at the Weather Prediction Center from 2001 to
510 2011. *Weather Forecast.*, 29, 894–911, 2014.
- 511 Walters, D., and Coauthors: The Met Office Unified Model Global Atmosphere 6.0/6.1 and
512 JULES Global Land 6.0/6.1 configurations. *Geosci. Model Dev.*, 10, 1487–1520, 2017
- 513 Webster S., Brown, A.R., Cameron, D. and Jones, C.P. : Improvements to the representation of
514 orography in the Met Office Unified Model. *Q. J. R. Meteorol. Soc.*, 126, 1989–2010, 2003
515
- 516 Wilks, D.S. (Eds.) : Statistical Methods in the Atmospheric Sciences. 3rd Edition. Elsevier, 676
517 pp., 2011
518
- 519 Wilson, C. : Review of current methods and tools for verification of numerical forecasts of
520 precipitation. *Technical Report WP2.1*, UK Met Office, 2000.
- 521 Wood, N., and Coauthors : An inherently mass-conserving semi-implicit semi-Lagrangian
522 discretization of the deep atmosphere global non-hydrostatic equations. *Quart. J. Roy. Meteor.*
523 *Soc.*, 140, 1505–1520, 2014



524 Zhu, Y., Toth, Z., Wobus, R., Richardson, D. and Mylne, K.: The economic value of ensemble-
525 based weather forecasts. *Bull. Am. Meteorol. Soc.*, 83, 73–83, 2002

526 Zhu, K., Yang, Y., and Ming, X.: Percentile-based Neighborhood Precipitation Verification and
527 Its Application to a Land falling Tropical Storm Case with Radar Data Assimilation. *Adv. in*
528 *Atmos. Sc.*, 32, 1449–1459, 2015

529



530 *Table 1. Some of the important Unified Model (UM) changes in recent years.*

Year	UM Versions	Configurations	
		Resolution and Data Assimilation System	Dynamical Core
2007	UM6.4 (Feb), UM6.5 (July)	N320L50 (~40 km in mid-latitudes), 12 Minute time step, 4D-VAR data assimilation	New Dynamics (ND)
2008	UM7.0 (Mar), UM7.1 (Aug)	N320L50 (~40 km in mid-latitudes), 12 Minute time step, 4D-VAR data assimilation	
2009	UM7.3 (Mar), UM7.4 (Aug)	N320L70 (~40 km in mid-latitudes), 12 minute time step, 4D-VAR data assimilation	
2010	UM7.6 (Apr), UM7.1 (Aug)	N512L70 (~25 km in mid-latitudes), 10 minute time step, 4D-VAR data assimilation	
2011	UM7.9 (Apr), UM8.0 (Aug)	N512L70 (~25 km in mid-latitudes), 10 minute time step, Hybrid 4D-VAR data assimilation	
2012	UM8.2 (Apr, PS29), UM8.2 (Sept, PS30)	N512L70 (~25 km in mid-latitudes), 10 minute time step, Hybrid 4D-VAR data assimilation	
2013	UM8.2 (Jan , PS31), UM8.2 (Apr, PS32)	N512L70 (~25 km in mid-latitudes), 10 minute time step, Hybrid data assimilation	
2014	UM8.4 (Feb, PS33)	N512L70 (~25 km in mid-latitudes), 10 minute time step, Hybrid 4D-VAR data assimilation	Even Newer Dynamics for General Atmospheric Modeling of the environment (ENDGame)
	UM8.5 (July, PS34)	N768L70 (~17 km in mid-latitude), 7.5 minute time step, Hybrid 4D-VAR data assimilation	
2015	UM 8.5(Feb, PS35) UM 10.1(Aug, PS36)	N768L70 (~17 km in mid-latitude), 7.5 minute time step, Hybrid 4D-VAR data assimilation	
2016	UM 10.2(Mar, PS37) UM10.4 (Nov, PS38)	N768L70 (~17 km in mid-latitude), 7.5 minute time step,	
2017	UM10.6 (Jul, PS39)	N1280L70 (~10km in Mid-latitude), 4 minute time step, Hybrid 4D-VAR data assimilation	
2018	UM10.8 (Feb, PS40) UM10.9 (Sep,PS41)	N1280L70 (~10km in Mid-latitude), 4 minute time step, Hybrid 4D-VAR data assimilation	



531 *Table 2: Contingency table representing the frequencies of forecast-observation*
 532 *pairs for which the event and non-event were forecasted and observed*

		<i>Observed</i>		
		<i>Yes</i>	<i>No</i>	<i>Total</i>
<i>Forecast</i>	<i>Yes</i>	Hits(a)	False alarms(b)	Forecast yes
	<i>No</i>	Missed(c)	Correct negatives(d)	Forecast no
<i>Total</i>		Observed yes	Observed no	total

533
 534

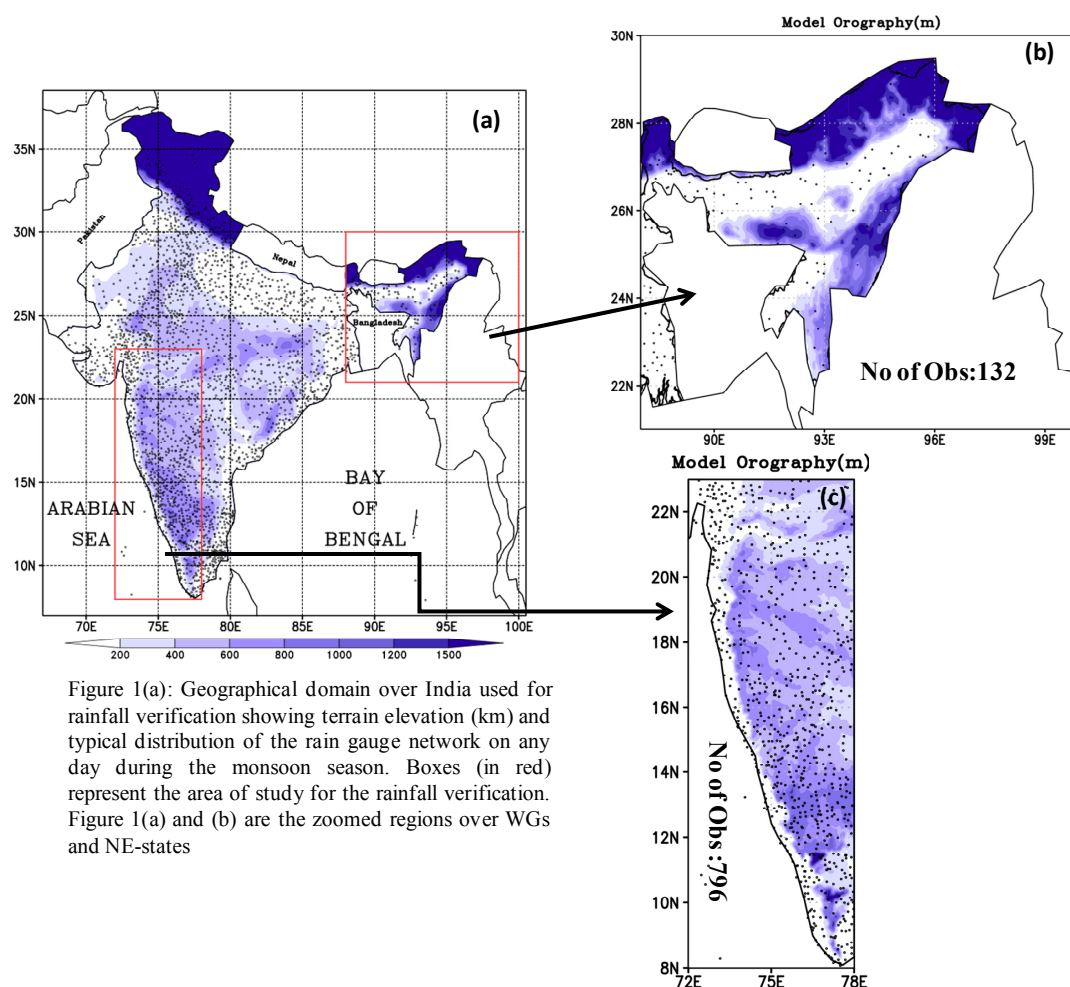


535 *Table3. Categorical scores used in rainfall forecast verification in the present study*

NAME	ACRONYMS and DEFINITIONS
BIAS	$BIAS = \frac{a+b}{a+c}$
Probability of Detection	$POD = \frac{a}{a+c}$ also known as Hit Rate (H)
False Alarm Ratio	$FAR = \frac{b}{a+b}$
Probability of False Detection	$POFD = \frac{b}{b+d}$ or known as False Alarm Rate (F)
Critical Success Index	$CSI = \frac{a}{a+b+c}$ also known as Threat Score (TS)
Symmetric EDI	$SEDI = \frac{\ln F - \ln H + \ln(1-H) - \ln(1-F)}{\ln F + \ln H + \ln(1-H) + \ln(1-F)}$ Where H is hit rate and F is False Alarm Rate



536



537

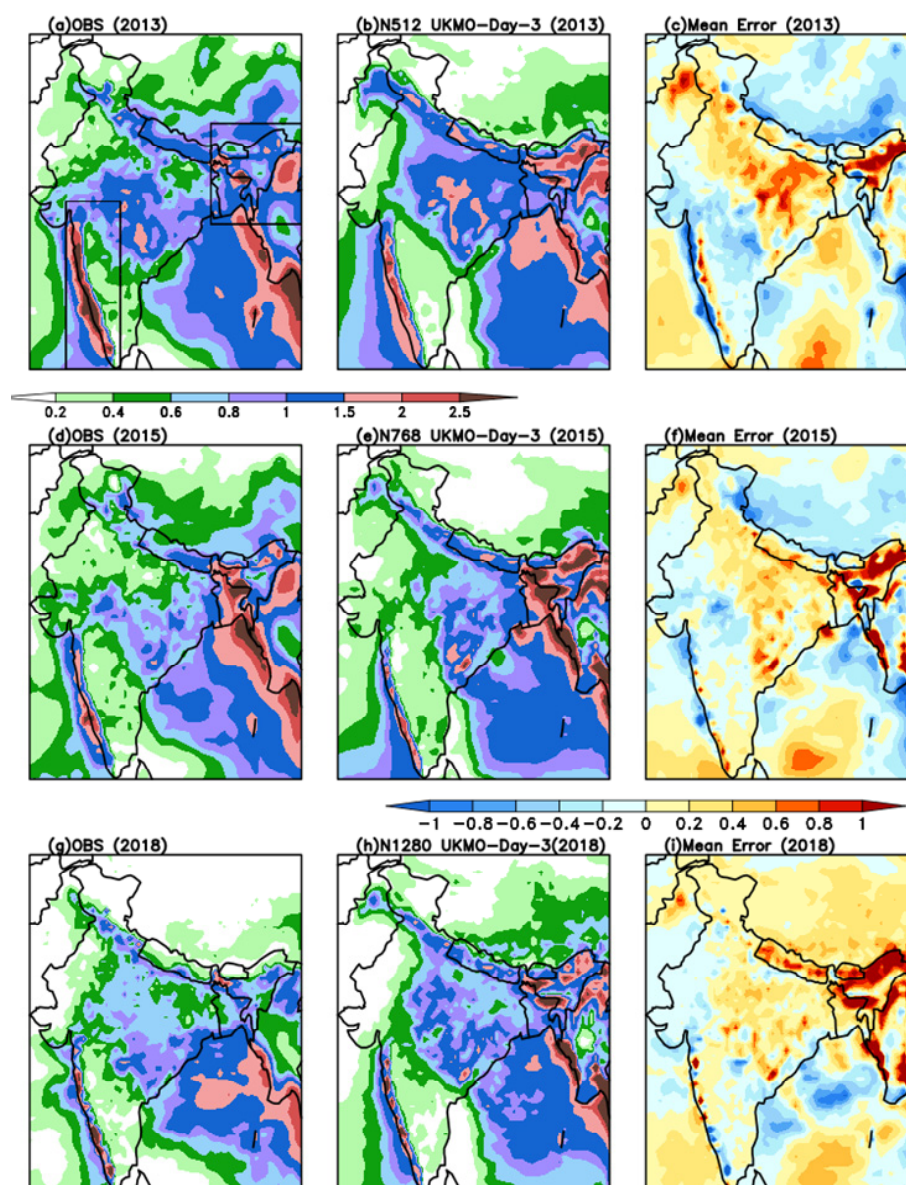
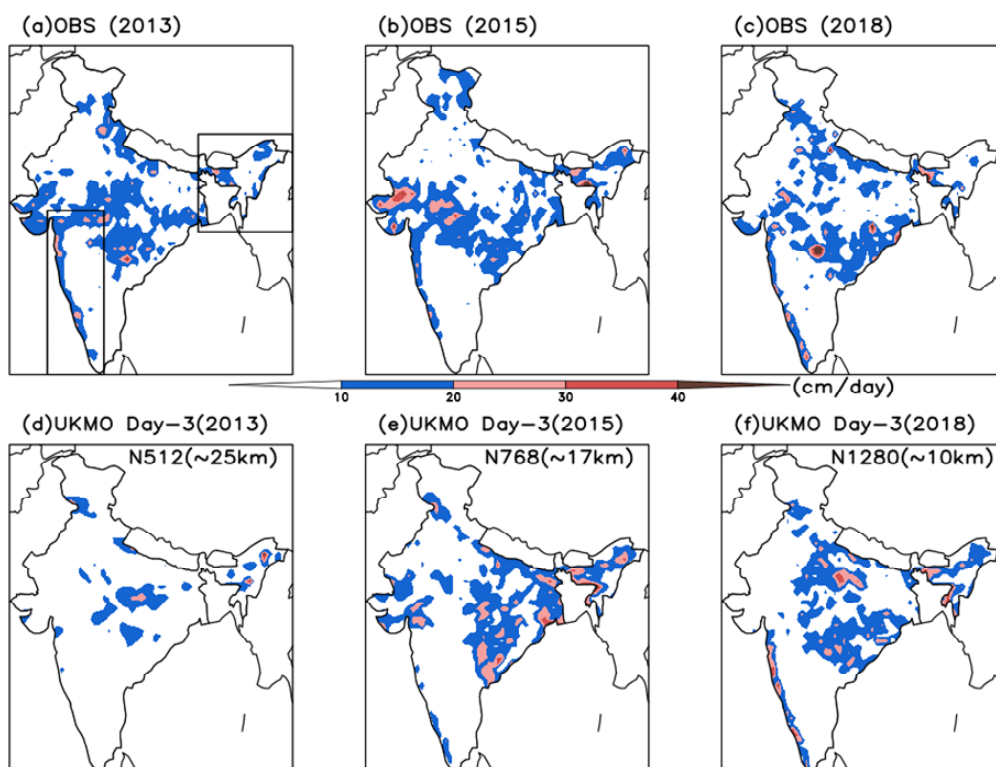


Figure 2. Observed (left panel), Day-3 Forecast mean rainfall (middle panel) and Mean Error (right panel) in cm day^{-1} over India during JJAS 2013, 2015 and 2018.



540

Figure 3. Observed (upper panel) and UKMO Day-3 highest rainfall Forecast (lower panel) at each grid point during JJAS 2013 , 2015 and 2018

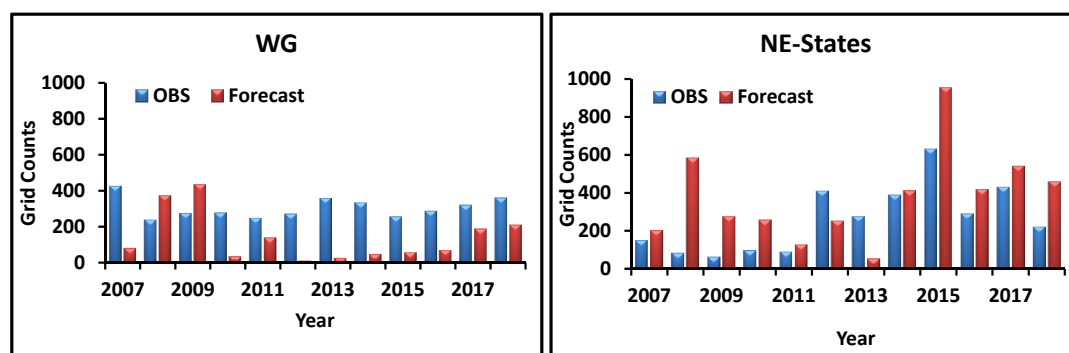
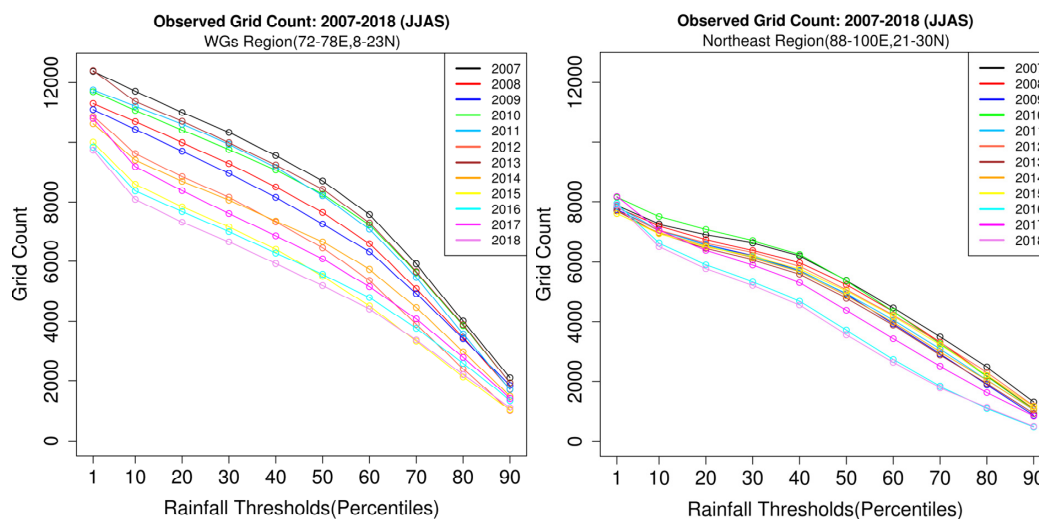


Figure 4. Number of counts in the observed and Day-3 forecast of rainfall threshold of 10cm/day over (a) WGs (b) NE-states



544

545

Figure 5. Observed rainfall counts over the WG and NE-states during JJAS 2007-2018.

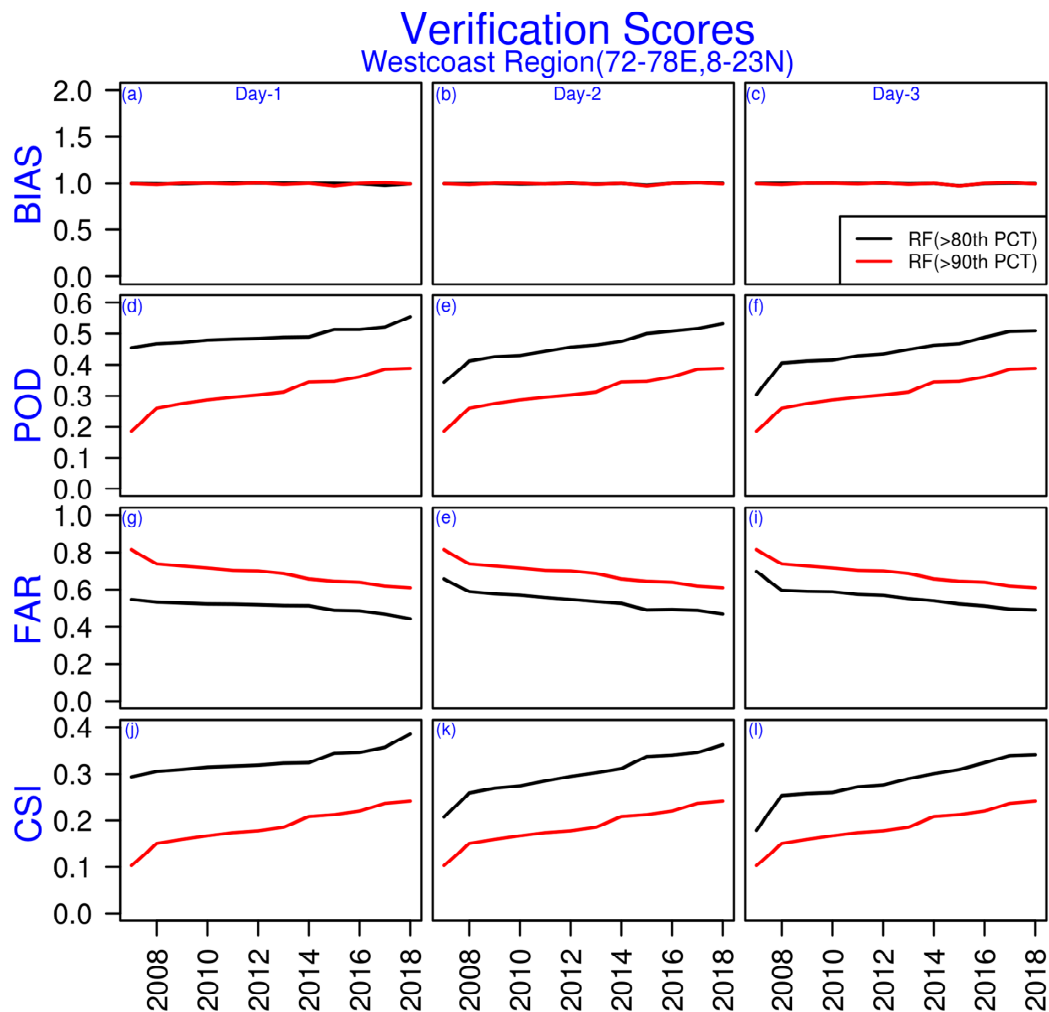


Figure 6. Bias (a-c), Probability of Detection (POD; (d-f)), False alarm Ratio (FAR;(g-i)) and Critical success index (CSI;(j-l)) computed for Day-1 Day-2 and Day-3 forecasts for CAT1 and CAT2 rainfall thresholds during JJAS 2007-2018 over WG .

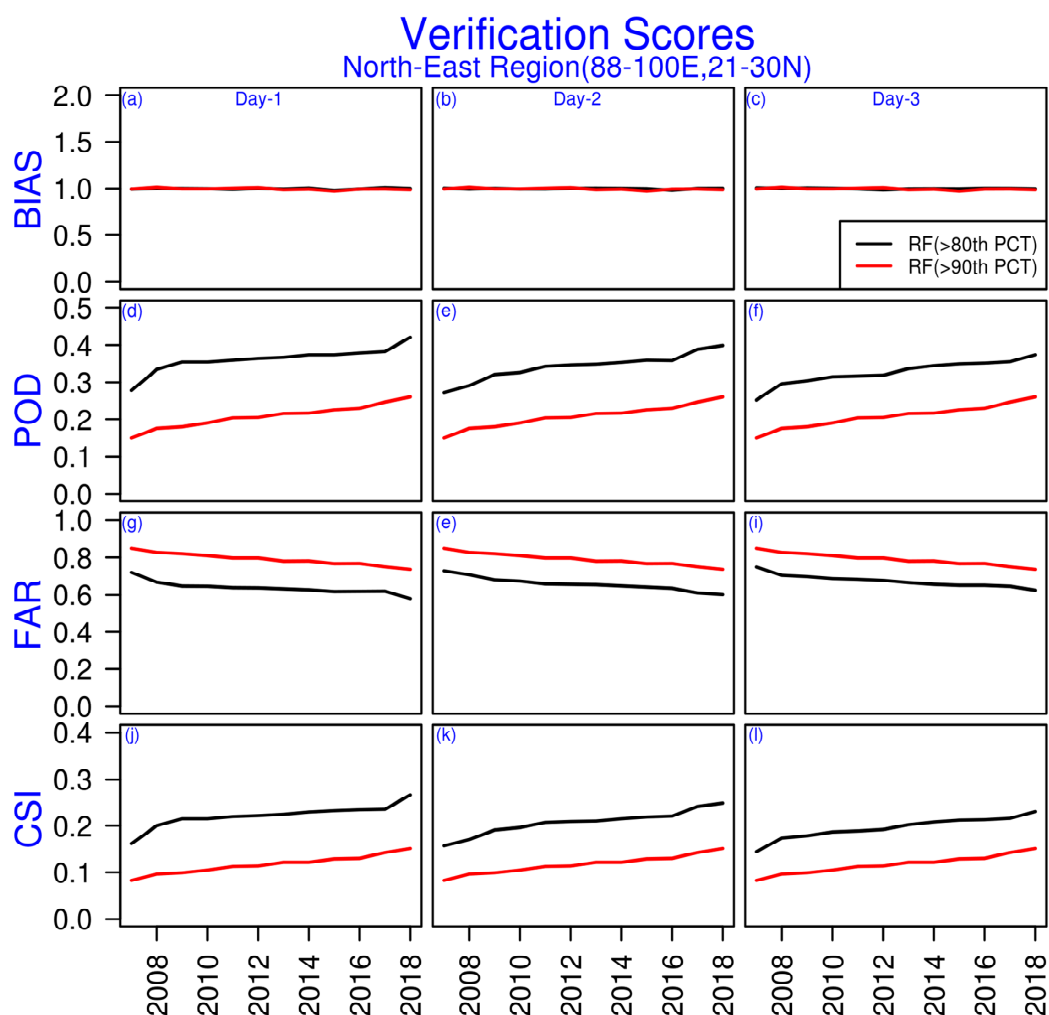


Figure 7. Bias (a-c), Probability of Detection (POD; (d-f)), False alarm Ratio (FAR;(g-i)) and Critical success index (CSI;(j-l)) computed for Day-1 Day-2 and Day-3 forecasts for CAT1 and CAT2 rainfall thresholds during JJAS 2007-2018 over NE-states .

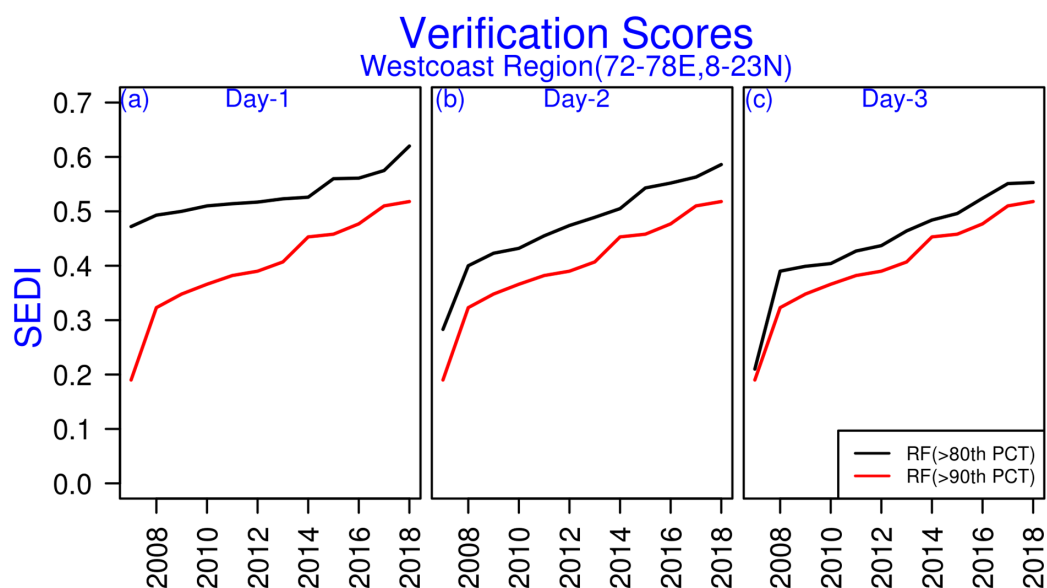


Figure 8. Symmetric extremal Dependence Index (EDI; (a-c))) computed for Day-1 Day-2 and Day-3 forecasts for CAT1 and CAT2 rainfall thresholds during JJAS 2007-2018 over WG region

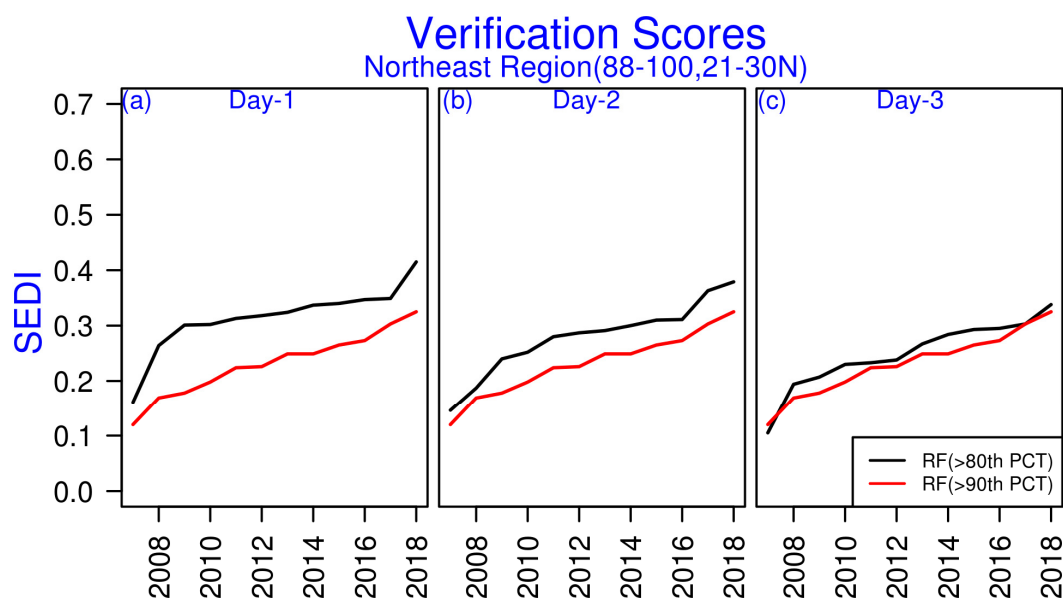


Figure 9. Symmetric extremal Dependence Index (EDI; (a-c)) computed for Day-1 Day-2 and Day-3 forecasts for CAT1 and CAT2 rainfall thresholds during JJAS 2007-2018 over NE-states